

2006

Skyrmion-like excitations in dynamical lattices

PG Kevrekidis

University of Massachusetts - Amherst, kevrekid@math.umass.edu

Follow this and additional works at: http://scholarworks.umass.edu/math_faculty_pubs



Part of the [Physical Sciences and Mathematics Commons](#)

Kevrekidis, PG, "Skyrmion-like excitations in dynamical lattices" (2006). *Mathematics and Statistics Department Faculty Publication Series*. Paper 1073.

http://scholarworks.umass.edu/math_faculty_pubs/1073

This Article is brought to you for free and open access by the Mathematics and Statistics at ScholarWorks@UMass Amherst. It has been accepted for inclusion in Mathematics and Statistics Department Faculty Publication Series by an authorized administrator of ScholarWorks@UMass Amherst. For more information, please contact scholarworks@library.umass.edu.

Skyrmion-like excitations in dynamical lattices

P. G. Kevrekidis¹, R. Carretero-González², D. J. Frantzeskakis³, B. A. Malomed⁴, and F. K. Diakonov³

¹ *Department of Mathematics and Statistics, University of Massachusetts, Amherst MA 01003-4515*

² *Nonlinear Dynamical Systems Group, San Diego State University, San Diego CA, 92182-7720*

³ *Department of Physics, University of Athens, Panepistimiopolis, Zografos, Athens 15784, Greece*

⁴ *Department of Interdisciplinary Studies, Faculty of Engineering, Tel Aviv University, Tel Aviv 69978, Israel*

We construct discrete analogs of Skyrmions in nonlinear dynamical lattices. The Skyrmion is built as a vortex soliton of a complex field, coupled to a dark radial soliton of a real field. Adjusting the Skyrmion ansatz to the lattice setting allows us to construct a *baby-Skyrmion* in two dimensions (2D) and extend it into the 3D case (1D counterparts of the Skyrmions are also found). Stability limits for these patterns are obtained analytically and verified numerically. The dynamics of unstable discrete Skyrmions is explored, and their stabilization by external potentials is discussed.

Introduction. Recently, studies of intrinsic localized modes (ILMs) in nonlinear lattice systems have drawn much attention [1] due to their relevance to various physical problems including, *inter alia*, optical waveguide arrays [2], photonic crystals [3], Bose-Einstein condensates (BECs) trapped in deep optical lattices (OLs) [4], and Josephson-junction ladders [5].

A wide variety of self-supporting ILM type of excitations have been predicted theoretically and observed experimentally. Prominent examples are bright and dark optical discrete solitons [6, 7] in AlGaAs waveguide arrays [7], multi-dimensional solitons in photonic lattices [8, 9, 10], discrete vortex solitons [11, 12, 13], lattice dipole solitons [14], multi-component solitons [15], soliton trains [16], necklace solitons [17], and so on. Parallel to these achievements in optics, a remarkable recent result was the creation of gap solitons in BECs loaded in OLs [18]. In fact, BECs offer an interesting implementation of nonlinear dynamics in *confined lattices*, due to the fact that experiments are always run in an external trap [4]. These developments raise the question whether counterparts of more complex structures, that were originally proposed in continuum media within field-theoretical contexts, can be predicted and observed in dynamical lattices.

Among the most fundamental objects of this type are the three-dimensional (3D) Skyrmions, initially proposed to explain topologically the origin of the baryon quantum number [19]. On the other hand, their two-dimensional (2D) version, so-called “baby-Skyrmions”, were used to model bubble generation in condensed-matter systems in the presence of an external magnetic field. In particular, baby-Skyrmions seem to have a central role in the disappearance of antiferromagnetism and the onset of high- T_c superconductivity [20], as well as in the ground state properties of the quantum Hall ferromagnets [21]. Recently, stable Skyrmions have also been predicted in BECs [22]. On the other hand, as concerns *discrete* systems, stable discrete Skyrmions on lattices were considered in the framework of the Heisenberg model for magnetism [23], as well as in the 2D Hubbard model [24]. Additionally, Skyrme lattices are also very interesting due to their ability to describe electron spin textures in quan-

tum Hall systems [25]. Importantly, discrete Skyrmions play also an essential role for the quantization of the original Skyrme model [26], the continuum version of which is non-renormalizable.

In the present work, we discuss the discretization of Skyrmions from a different point of view. Putting the continuity aspect on second priority, we develop discrete solitons with topological properties equivalent to those of Skyrmions in the continuum field theory. We show that the proposed Skyrmion-like structures (for simplicity called “Skyrmions” hereafter) can be stabilized on the dynamical lattice under consideration, namely a nonlinear Schrödinger lattice.

We aim to construct discrete Skyrmion states in a paradigmatic nonlinear-lattice model, *viz.*, the discrete nonlinear Schrödinger (DNLS) equation. DNLS is a universal envelope wave equation for a variety of Hamiltonian systems (such as, e.g., nonlinear Klein-Gordon lattice models), and, moreover, is a direct model for BECs trapped in strong OLs [4] and crystals built of microresonators [27]; in addition, its 2D version models optical waveguide arrays [2, 6]. As Skyrmions necessarily involve (through the so-called *hedgehog ansatz* [28, 29]) *three* scalar fields, and are characterized by two independent topological charges, their description requires two complex field variables. Thus, in this work we study a two-component DNLS equation. This model is directly relevant to waveguide arrays [15], when the light has different polarizations or frequencies, and to binary BECs composed as spin state mixtures of the same isotope [30].

The paper is structured as follows: In the next section, we present the model and some analytical considerations. Then, we report numerical results for 1D, 2D, and 3D lattices, and, finally, we summarize our findings.

Model and Analytics. We consider a vector DNLS equation for $\phi \equiv (\phi_1, \phi_2)^T$ on the cubic/square lattice,

$$i\dot{\phi}_{\mathbf{n}} = -C\Delta^{(d)}\phi_{\mathbf{n}} + (\phi^T G \phi)\phi, \quad G = \begin{pmatrix} 1 & 0 \\ 0 & \beta \end{pmatrix}, \quad (1)$$

where overdot stands for derivative in time (or, in the optical-waveguide model, in the propagation distance), C is a coupling constant, the parameter β characterizes the intra-species interaction, and the D -dimensional discrete

Laplacian is $\Delta^{(D)}\phi_{\mathbf{n}} \equiv \sum_{\mathbf{m}=\langle \mathbf{n} \rangle} \phi_{\mathbf{m}} - 2D\phi_{\mathbf{n}}$, with $\langle \mathbf{n} \rangle$ standing for the nearest-neighbor shell of \mathbf{n} [the latter is a vector index in the D -dimensional case — e.g., $\mathbf{n} = (n_1, n_2, n_3)$ in 3D]. Stationary solutions are looked for as $\phi_{\mathbf{n}} = \exp(-i\Lambda t)(u_{\mathbf{n}}, v_{\mathbf{n}})^T$, where Λ is the frequency (or chemical potential in the context of BECs), and $u_{\mathbf{n}}, v_{\mathbf{n}}$ obey the following equations

$$\Lambda u_{\mathbf{n}} = -C\Delta u_{\mathbf{n}} + (|u_{\mathbf{n}}|^2 + \beta|v_{\mathbf{n}}|^2)u_{\mathbf{n}}, \quad (2)$$

$$\Lambda v_{\mathbf{n}} = -C\Delta v_{\mathbf{n}} + (|v_{\mathbf{n}}|^2 + \beta|u_{\mathbf{n}}|^2)v_{\mathbf{n}}. \quad (3)$$

Note that the nonlinear-interaction matrix G in Eq. (1) implies self-repulsion of the lattice field, while the model with self-attraction, i.e., G replaced by $-G$, can be transformed into the present form by the known *staggering transformation*; for instance, $(u_{\mathbf{n}}, v_{\mathbf{n}}) \equiv (-1)^{n_1+n_2+n_3}(\tilde{u}_{\mathbf{n}}, \tilde{v}_{\mathbf{n}})$ in the 3D case.

We first construct solutions with the desired structures in the so-called anti-continuum (AC) limit of $C = 0$, and then continue solution branches to $C > 0$, by means of a fixed-point iteration converging to the relevant solutions. Once these have been obtained, linear-stability analysis is performed for a perturbed solution, $\phi_{\mathbf{n}}^{(\text{pert})} = (\phi_{\mathbf{n}} + \mathbf{a}_{\mathbf{n}}e^{\lambda t} + \mathbf{b}_{\mathbf{n}}e^{\lambda^* t})e^{-i\Lambda t}$, where $\mathbf{a}_{\mathbf{n}}$ and $\mathbf{b}_{\mathbf{n}}$ constitute an eigenmode of infinitesimal perturbations, and λ is the corresponding eigenvalue. The stationary solution is unstable if at least one pair of λ has nonzero real part.

We start with the 2D case, where the baby-Skyrmion can be found in the continuum model, using a ‘‘hedgehog’’ ansatz (in the polar coordinates) [28, 29], namely

$$\Psi = [\sin(f(r))\cos(k\theta), \sin(f(r))\sin(k\theta), \cos(f(r))]^T, \quad (4)$$

subject to the boundary conditions $\lim_{r \rightarrow 0} f(r) = M\pi$, and $\lim_{r \rightarrow \infty} f(r) = N\pi$, with integer k, M and N . The winding number of the corresponding state is $[(-1)^N - (-1)^M]k/2$. We will try to construct a counterpart of ansatz (4) on the 2D lattice. In particular, combining the first two components of ansatz (4) as $\Psi_1 + i\Psi_2$, we obtain a complex field with vorticity k . To consider the fundamental Skyrmions, we set $k = 1$ and $M = 0, N = 1$. Accordingly, the complex field is a localized discrete vortex, while the remaining field may be real, taking the form of a dark soliton in the (quasi-)radial direction on the lattice. For $C = 0$, one can construct a discrete vortex (alias *vortex cross*) by assigning the complex fields phases $0, \pi/2, \pi, 3\pi/2$ and modulus $\sqrt{\Lambda}$ at four sites, $(m, n) = (1, 0), (0, 1), (-1, 0)$ and $(0, -1)$, which surround the central point [11]. The radial dark soliton in the real field is achieved, in the same AC limit, by setting $v_{0,0} = 1$ and $v_{m,n} = -1$ at all other sites, with the exception of the above-mentioned four sites surrounding the origin, where $v_{m,n} = 0$. Notice that this corresponds to a hedgehog ansatz with $f(0) = 0, f(1) = \pi/2$ and $f(r > 1) = \pi$. Of course, the size of the vortex structure may be made larger in the AC limit, but this adversely affects the stability of the vortex [31], therefore we do not examine such cases here.

We note that the above 2D structure suggests a 1D analog of the Skyrmion, essentially as a cross-section of the 2D profile. In particular, in the AC limit, the 1D configuration becomes $u_n = \sqrt{\Lambda}(\delta_{n,1} - \delta_{n,-1}), v_0 = \sqrt{\Lambda}, v_1 = v_{-1} = 0$ and $v_n = -\sqrt{\Lambda}$ for $|n| > 1$. This 1D structure essentially consists of a twisted localized mode [32] in the one field, coupled to a pair of discrete dark solitons in the other. A variety of generalizations to the 3D case, resulting from Skyrmion’s rotation, are possible, but we limit our considerations to the simplest setting where $u_{\mathbf{n}}$ is a planar excitation (as above) with the well-defined vorticity around the third dimension, while $v_{0,0,0} = \sqrt{\Lambda}$, the field vanishes at the immediate neighbors of $(0, 0, 0)$ and has a value of $-\sqrt{\Lambda}$ elsewhere.

To examine instabilities relevant to the discrete Skyrmion, we first examine the dispersion relation for the equations linearized around such a solution (i.e., the continuous spectrum). While the full spectrum also contains isolated eigenvalues, it is its continuous component which is primarily responsible for instabilities (see below). Thus, we perturb the asymptotic lattice field, far from the Skyrmion’s center, as follows:

$$\phi_1 = \epsilon A e^{i(\omega t + kn)} + \epsilon B e^{-i(\omega^* t + kn)}, \quad (5)$$

$$\phi_2 = -1 + \epsilon C e^{i(\omega t + kn)} + \epsilon D e^{-i(\omega^* t + kn)}. \quad (6)$$

Using Eqs. (5)-(6) in Eq. (1) yields two excitation branches, associated, respectively, with the zero and non-vanishing backgrounds of the first and second fields,

$$\omega = \pm [\Lambda - \beta - 4CD \sin^2(k/2)], \quad (7)$$

$$\omega = \pm \sqrt{\Lambda + 4CD \sin^2(k/2) - \Lambda^2}, \quad (8)$$

which restricts the relevant spectral bands to $\pm[\Lambda - \beta - 4CD, \Lambda - \beta]$ and $[-\sqrt{(\Lambda + 4CD)^2 - \Lambda^2}, \sqrt{(\Lambda + 4CD)^2 - \Lambda^2}]$. These bands have opposite *Krein signatures* [33], hence their collision, occurring with the increase of C , at

$$C_{\text{cr}}^{(D)} = (\beta - \Lambda)^2 / [8D(2\Lambda - \beta)], \quad (9)$$

will generate complex eigenvalues, i.e., instability. Thus, the discrete Skyrmions may only be stable in the interval of $0 \leq C < C_{\text{cr}}^{(D)}$; in particular, for $C_{\text{cr}}^{(D)} > 0$ one requires $2\Lambda > \beta$. It is interesting to mention that $C_{\text{cr}}^{(D)} \rightarrow \infty$ (the continuum limit) as $\Lambda - \beta/2 \rightarrow +0$; however, analysis of this special case is beyond the scope of this paper.

Numerical Results. We first display numerical findings for the 1D case in Fig. 1. Shown are norms of the solution, $N_1 = \sum_{\mathbf{n}} |u_{\mathbf{n}}|^2$ and $N_2 = \sum_{\mathbf{n}} (\Lambda - |v_{\mathbf{n}}|^2)$, and most unstable eigenmodes and eigenvalues (computed on a lattice with 400 sites). In this case, Eq. (9) predicts $C_{\text{cr}}^{(1)} \approx 0.102083$, which coincides with the numerical finding (0.102 ± 0.0005). Examples of stable and unstable 1D Skyrmions are included too, for $C = 0.05$ and $C = 0.15$. As expected (see above), the destabilization occurs, indeed, via the collision of two continuous bands

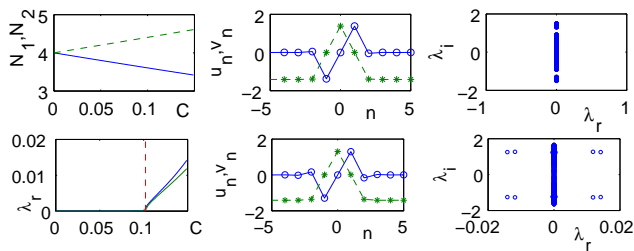


FIG. 1: (Color online) 1D discrete analog of the Skyrmion. Top and bottom panels in the left column show, respectively, norms N_1, N_2 (defined in the text) and two most unstable eigenmodes vs. coupling C [the vertical dashed line is the instability onset as predicted by Eq. (9)]. Upper and bottom panels in the middle and right columns display, respectively, the solution for $C = 0.05$ and $C = 0.15$, and the corresponding spectral planes (λ_r, λ_i) of the eigenvalue $\lambda = \lambda_r + i\lambda_i$.

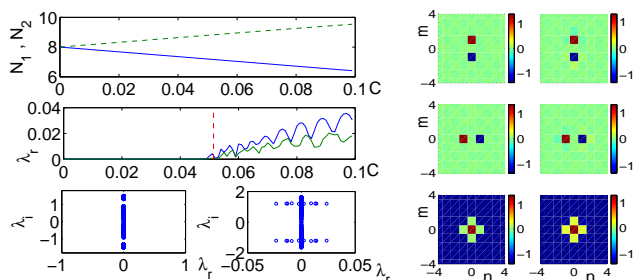


FIG. 2: (Color online) Same diagnostics as in Fig. 1 for discrete 2D (*baby-*) Skyrmions. Left and right paired panels pertain, respectively, to $C = 0.025$ and $C = 0.075$. Solution profiles are shown on the right, with the top, middle, and bottom rows displaying contours of real and imaginary parts of the first (complex) field, and the second (real) field.

of eigenvalues at the critical point. It has been checked that the numerical results, displayed here for $\Lambda = 2 = 8\beta$, adequately represent a large area in the parameter space.

Results for the 2D case are presented in Fig. 2. We again observe excellent agreement of the theoretical prediction (9) for the instability onset, at $C = C_{\text{cr}}^{(2)} = 0.051042$. Typical solution examples are shown for $C = 0.025$ (stable) and $C = 0.075$ (unstable).

An example of one of the possible (as mentioned above) 3D generalizations of the 2D discrete baby-Skyrmion is shown in Fig. 3. In this case, the complex field is arranged as a 3D soliton carrying a vortex in the horizontal plane (cf. Ref. [34]), while the real component features a 3D radial dark soliton. A stable 3D discrete Skyrmion is shown for $C = 0.01$ (in this case, $C_{\text{cr}}^{(3)} = 0.034028$).

The next step is to simulate the evolution of unstable solutions. As, beyond the primary instability threshold (9), a cascade of secondary instabilities is produced by additional collisions between the continuous spectral bands, one may expect that the corresponding multitude of unstable eigenmodes leads to a kind of lattice turbulence, especially because the unstable eigenmodes

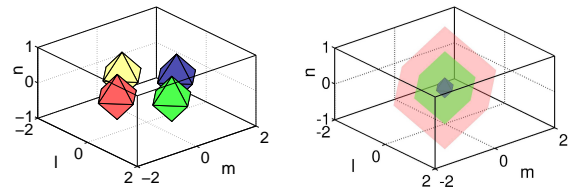


FIG. 3: (Color online) A 3D discrete Skyrmion for $C = 0.05$. The left and right panels show, respectively, contours of the first (complex) field, at $\text{Re}(\phi_1) = \pm 1$ (blue/red) and $\text{Im}(\phi_1) = \pm 1$ (green/yellow), and of the second (real) field, at $\phi_2 = (-1, 0, 1)$ (red, green and blue, respectively).

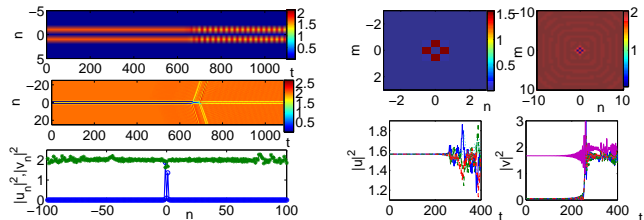


FIG. 4: (Color online) Instability development in one- and two-dimensional discrete Skyrmions. The top, middle, and bottom left panels show, respectively, space-time contours of the absolute value of the first (complex) field and of the second (real) one, and the spatial distribution of the fields at $t = 1100$ in the 1D case. The top right panels display the contours of the square modulus of the two fields for the 2D case, at the instability onset, $t = 220$, while the panels beneath them show the evolution of the fields at the central site and its four neighbors, for the same case.

are delocalized, as they belong to the continuous spectrum. Indeed, this is what we observe in direct simulations, as shown in Fig. 4 for $C = 0.149 > C_{\text{cr}}^{(1)}$ and $C = 0.099 > C_{\text{cr}}^{(2)}$ in the 1D and 2D cases. In the 1D case (the left part of the figure), the weakly unstable configuration remains undisturbed for a long time, but eventually, around $t \approx 650$, the instability generates spatial chaos in the real (second) field component, and breathing in its complex counterpart. This dynamics persists for long evolution times. Transition to chaotic behavior is also observed (in the right part of Fig. 4) in the 2D case, after the onset of the instability around $t = 220$.

Finally, we also considered the influence of external potentials, which is necessary in the application to BECs, that are typically confined by a parabolic trap. In the 1D case, the latter amounts to adding a term $(\Omega^2/2)n^2\phi$ to Eq. (1) (in the 2D and 3D cases, the trap produces qualitatively similar effects). As seen in Fig. 5, the profile of the v field now has a finite size, as per the Thomas-Fermi approximation [4]. The main novel feature induced by the trap is the appearance of *gaps* in the linearization spectrum, which leads to the dependence of the largest unstable eigenvalue on C , as shown in the top panel of Fig. 5. Interestingly, while the envelope of this dependence traces a curve similar to that in Fig. 1, the gaps

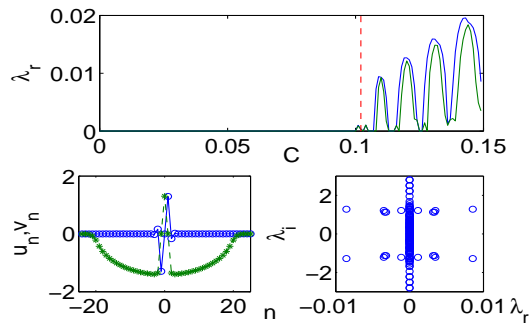


FIG. 5: (Color online) The most unstable eigenvalue (top) for the 1D lattice Skyrmion, and an example of the field configuration and its stability for $C = 0.15$ (bottom left and right) in the presence of the confining parabolic potential with $\Omega = 0.1$.

lead to *restabilization* of the discrete Skyrmion in certain intervals. For instance, the solution shown is stable for $0.113 \leq C \leq 0.115$, where it is unstable without the trap. Hence, the parabolic potential offers (which is also true in the 2D and 3D cases) an additional mechanism of stabilization of the discrete Skyrmions.

Conclusions. We have constructed discrete structures

that emulate Skyrmions on nonlinear dynamical lattices. We have used the “hedgehog” ansatz for 2D (*baby*-) Skyrmions in continuum field models as a guide towards constructing the lattice solutions and extending them to both 3D and 1D settings. Generally, the lattice Skyrmion is built herein as a vortex soliton in a complex field coupled to a dark radial soliton in a coupled real field. We have predicted stability limits of the lattice Skyrmions and identified the principal mechanism of their destabilization. The analytical prediction was verified by numerical computations, that corroborate the *stability* of the Skyrmions in the predicted region. We have also demonstrated that the evolution of unstable discrete Skyrmions leads to onset of lattice turbulence. A possibility of further stabilization of the Skyrmions by means of an external confining potential was highlighted too.

It would be interesting to examine analogs of the structures presented herein with higher values of the topological charge, as well as more complex patterns in 3D. Creation of the lattice Skyrmions in binary BECs mixtures trapped in a deep optical lattice by means of available techniques appears to be within experimental reach.

-
- [1] S. Aubry, *Physica* **103D**, 201 (1997); S. Flach and C. R. Willis, *Phys. Rep.* **295**, 181 (1998); D. K. Campbell *et al.*, *Phys. Today*, January 2004, p. 43.
- [2] A.A. Sukhorukov *et al.*, *IEEE J. Quant. Elect.* **39**, 31 (2003); U. Peschel *et al.*, *J. Opt. Soc. Am. B* **19**, 2637 (2002).
- [3] S. F. Mingaleev and Y. S. Kivshar, *Phys. Rev. Lett.* **86**, 5474 (2001).
- [4] A. Trombettoni and A. Smerzi, *Phys. Rev. Lett.* **86**, 2353 (2001); F. Kh. Abdullaev *et al.*, *Phys. Rev.* **A64**, 043606 (2001); F. S. Cataliotti *et al.*, *Science* **293**, 843 (2001); A. Smerzi *et al.*, *Phys. Rev. Lett.* **89**, 170402 (2002); G. L. Alfimov *et al.*, *Phys. Rev. E* **66**, 046608 (2002); R. Carretero-González and K. Promislow, *Phys. Rev. A* **66** 033610 (2002).
- [5] P. Binder *et al.*, *Phys. Rev. Lett.* **84**, 745 (2000); E. Trías *et al.*, *Phys. Rev. Lett.* **84**, 741 (2000).
- [6] D. N. Christodoulides *et al.*, *Nature* **424**, 817 (2003); P. G. Kevrekidis *et al.*, *Int. J. Mod. Phys. B* **15**, 2833 (2001).
- [7] H. S. Eisenberg *et al.*, *Phys. Rev. Lett.* **81**, 3383 (1998); R. Morandotti *et al.*, *Phys. Rev. Lett.* **86**, 3296 (1999).
- [8] J. W. Fleischer *et al.*, *Phys. Rev. Lett.* **90**, 023902 (2003); *Nature* **422**, 147 (2003).
- [9] D. Neshev *et al.*, *Opt. Lett.* **28**, 710 (2003).
- [10] H. Martin *et al.*, *Phys. Rev. Lett.* **92**, 123902 (2004).
- [11] B.A. Malomed and P. G. Kevrekidis, *Phys. Rev. E*, **64**, 026601 (2001); B. B. Baizakov *et al.*, *Europhys. Lett.* **63**, 642 (2003); J. Yang and Z. Musslimani, *Opt. Lett.* **28**, 2094 (2003).
- [12] D. N. Neshev *et al.*, *Phys. Rev. Lett.* **92**, 123903 (2004).
- [13] J. W. Fleischer *et al.*, *Phys. Rev. Lett.* **92**, 123904 (2004).
- [14] J. Yang *et al.*, *Opt. Lett.* **29**, 1662 (2004).
- [15] J. Meier *et al.*, *Phys. Rev. Lett.* **91**, 143907 (2003).
- [16] Z. Chen *et al.*, *Phys. Rev. Lett.* **92**, 143902 (2004).
- [17] J. Yang *et al.*, *Phys. Rev. Lett.* **94**, 113902 (2005).
- [18] B. Eiermann *et al.*, *Phys. Rev. Lett.* **92**, 230401 (2004).
- [19] T. Skyrme, *Proc. Roy. Soc. London A* **260**, 127 (1961).
- [20] F. Wilczek, *Fractional Statistics and Anyon Superconductivity*, World Scientific, Singapore, 1990.
- [21] D.-H. Lee and C. L. Kane, *Phys. Rev. Lett.* **64**, 1313 (1990); S. L. Sondhi *et al.*, *Phys. Rev. B* **47**, 16419 (1993).
- [22] J. Ruostekoski and J. R. Anglin, *Phys. Rev. Lett.* **86**, 3934 (2001); U. Al. Khawaja and H. T. C. Stoof, *Nature (London)* **411**, 918 (2001); R. A. Battye *et al.*, *Phys. Rev. Lett.* **88**, 80501 (2002); C. M. Savage and J. Ruostekoski, *Phys. Rev. Lett.* **91**, 010403 (2003).
- [23] R. S. Ward, *Lett. Math. Phys.* **35**, 385 (1995).
- [24] G. Seibold, *Phys. Rev. B* **58**, 15520 (1998).
- [25] C. Timm *et al.*, *Phys. Rev. B* **58**, 10634 (1998).
- [26] A. J. Schramm and B. Svetitsky, *Phys. Rev. D* **62**, 114020 (2000).
- [27] J. E. Heebner and R. W. Boyd, *J. Mod. Opt.* **49**, 2629 (2002); P. Chak *et al.*, *Opt. Lett.* **28**, 1966 (2003).
- [28] T. Weidig, hep-th/9911056.
- [29] A. Kudryavtsev *et al.*, *Nonlinearity* **11**, 783 (1998).
- [30] D. S. Hall *et al.*, *Phys. Rev. Lett.* **81**, 1539 (1998).
- [31] D.E. Pelinovsky *et al.*, *Phys. D* **212**, 20 (2005).
- [32] S. Darmanyan *et al.*, *Sov. Phys. JETP* **86**, 682 (1998).
- [33] T. Kapitula *et al.*, *Physica D* **195**, 263 (2004).
- [34] P. G. Kevrekidis *et al.*, *Phys. Rev. Lett.* **93**, 080403 (2004).